

Proton resonances in ^{34}Cl from $E_x = 6.3$ to 8.8 MeV

J. R. Vanhoy,* E. G. Bilpuch, and C. R. Westerfeldt

Duke University, Durham, North Carolina 27706

and Triangle Universities Nuclear Laboratory, Duke Station, Durham, North Carolina 27706

G. E. Mitchell

North Carolina State University, Raleigh, North Carolina 27695

and Triangle Universities Nuclear Laboratory, Duke Station, Durham, North Carolina 27706

(Received 21 June 1989)

The $^{33}\text{S}(p,p_0)$, (p,p_1) , and (p,p_2) differential cross sections were measured in the energy range $E_p = 1.20$ – 3.77 MeV with an average overall energy resolution of 350 eV full width at half maximum. Resonance parameters were extracted for 144 levels with a multilevel, multichannel R -matrix code; parameters include resonance energy, total angular momentum, proton partial widths, and channel spin and orbital angular momentum mixing ratios. The $l = 1$ strength function is more than an order of magnitude larger than the $l = 0$ strength function. Most of the $l = 1$ strength is below $E_p \approx 2.6$ MeV and most of the $l = 0$ strength is above $E_p \approx 2.4$ MeV.

I. INTRODUCTION

The addition of a proton to ^{33}S forms the odd-odd $N = Z$ compound system ^{34}Cl . We have previously studied two other similar nuclei (^{26}Al and ^{30}P) via the (p,p) reaction.^{1,2} These nuclei are important for such topics as stretched particle-hole states and astrophysical reaction rates, as well as for nuclear structure calculations. Since the proton separation energy is very small ($S_p = 5.14$ MeV), the compound system is formed at low excitation energy. Thus for ^{34}Cl it may be possible to obtain the complete level scheme from the ground state to the resonance region. Levels at lower energies in ^{34}Cl have been studied by several reactions.^{3,4} The transfer reaction $^{33}\text{S}(^3\text{He},d)^{34}\text{Cl}$ was used by Erskine *et al.*⁵ to measure the spectroscopic factors of 26 levels up to $E_x = 4.7$ MeV. Brunnader *et al.*⁶ used the pickup reactions $^{36}\text{Ar}(p,^3\text{He})^{34}\text{Cl}$ and $^{36}\text{Ar}(d,\alpha)^{34}\text{Cl}$ to identify $T = 1$ states in ^{34}Cl and to study the J dependence of Coulomb displacement energies in the mass 34 system. Resonances have been studied almost completely by the proton capture reaction,^{7–10} although Dassie *et al.*¹¹ measured a few proton elastic scattering resonances.

A complete level scheme for ^{34}Cl from the ground state to the resonance region could be important for tests of statistical theory. The Gaussian orthogonal ensemble (GOE) version of random matrix theory has been very successful in describing the fluctuations of level spacings observed in neutron and proton scattering resonances.^{12,13} However, the status of spectrum fluctuations for low-lying states in nuclei is not clearly established. There is some evidence^{14–16} that the nearest-neighbor spacing distribution for the low-lying states is often intermediate between the GOE prediction (Wigner distribution) and the Poisson distribution. The fluctuation properties may depend on the symmetry of the states involved, i.e., on the type of nucleus considered. These analyses suffer from the limitation that only a very few

low-lying states of the same spin and parity are identified in each nucleus. An ideal analysis would include many states with the same J and π , covering the entire energy range from the ground state to the resonance region. The best approximation to this ideal is ^{26}Al , where the first 100 positive-parity states have been located and their J , π , and T values assigned.¹⁷ Analysis¹⁸ of these data indicates that the spacing fluctuations for all levels (from 0 to 8 MeV) obey GOE predictions. It would be very interesting to have such a complete level scheme for other nuclei. The crucial first step in an attempt to establish a complete level scheme for ^{34}Cl is the identification of the resonances in the (p,p) reaction. Detailed measurements of the γ -ray decay of these resonances can then be used to determine the properties of the bound states. This is the procedure applied successfully by Endt *et al.*¹⁷ in ^{26}Al .

Experimental procedures for the elastic scattering measurements are described in Sec. II. Analysis of the data to extract the resonance parameters is described in Sec. III. Level densities, resonance strengths, and the identification of analog states are discussed in Sec. IV. A brief summary is given in Sec. V.

II. EXPERIMENTAL PROCEDURE

The experiment was performed with the 4 MV Van de Graaff accelerator and associated high-resolution system at Triangle Universities Nuclear Laboratory (TUNL).¹⁹ This system provides proton beams from $E_p = 1$ to 4 MeV with an overall energy resolution of 300–400 eV for thin solid targets. The energy calibration is performed with secondary standard resonances: $^{44}\text{Ca}(p,p_0)^{44}\text{Ca}$ ($E_p = 1.8841$ MeV) and $^{56}\text{Fe}(p,p_0)^{56}\text{Fe}$ ($E_p = 3.2369$ MeV), determined with respect to the primary standard neutron thresholds $^7\text{Li}(p,n)^7\text{Be}$ at $E_p = 1.8804$ MeV and $^{13}\text{C}(p,n)^{13}\text{N}$ at $E_p = 3.2357$ MeV. The calibrations provide accurate energies (± 300 eV) near the calibration points and a maximum error of ± 1.5 keV away from the calibration points.

A major problem in studying the $^{33}\text{S}(p,p)^{33}\text{S}$ reaction was obtaining high enrichment sulfur in a chemical form convenient for preparing targets. Preliminary data were obtained with enriched CdS targets (88.2% ^{33}S) remaining from a previous experiment. These targets deteriorated in the proton beam, but were acceptable for an initial survey. Highly enriched ^{33}S now is difficult to obtain commercially. A small quantity (~ 10 mg) of elemental sulfur (88.2% ^{33}S , 11.0% ^{32}S , 0.8% ^{34}S) was obtained from Oak Ridge National Laboratory. Targets were prepared following a procedure similar to that utilized by Sterrenberg *et al.*²⁰ and by Nooren and van der Leun.²¹ Silver sulfide targets were prepared by first evaporating a thin layer of silver onto $5 \mu\text{g}/\text{cm}^2$ carbon backings on microscope slides. A suspension of ~ 1 mg sulfur in ~ 10 ml ethanol was prepared. The suspension was dripped onto warm silver-coated carbon foils and heated. The relative yields of the sulfur and silver peaks in the proton spectra were consistent with a target compound of Ag_2S . Thus the thickness of S could be controlled by the initial evaporation of Ag. These targets ($\sim 1 \mu\text{g}/\text{cm}^2$ of S) proved stable under $2\text{-}\mu\text{A}$ beam currents of 2-MeV protons. Targets which showed signs of decay were baked for an additional period to complete the chemical reaction. Even with these efforts target imperfections remained—the point scatter in the data is larger than estimated from counting statistics.

Data were obtained from $E_p = 1.20$ to 3.77 MeV in steps of 100–400 eV at laboratory angles of 90° , 108° , 135° , 150° , and 165° . Elastic scattering predominates, although two inelastically scattered proton groups (p_1 and p_2) are occasionally seen. The improved data obtained from these new targets allowed identification of many resonances which were not seen in the initial survey. A total of 144 resonances were observed, of which 54% are p -wave resonances. Very few s -wave resonances were observed below $E_p = 2.4$ MeV. At lower energies the resonances are fairly well isolated, but there are strong resonance interference effects in the middle and upper regions of the data. The analysis is complicated by a number of very large resonances (total width tens of keV).

III. RESONANCE ANALYSIS

Experimental excitation functions were fit with the multilevel, multichannel R -matrix program MULTI6, which is based on the formalism of Lane and Thomas.²² The program generates excitation functions for a given set of resonance parameters. A best visual fit is obtained by varying the resonance energies, spin and parities, angular momenta, and magnitudes and signs of all allowed reduced width amplitudes. Data at all angles and for all decay channels are fit simultaneously. A general description of the analysis procedure for nonzero spin targets was given by Nelson *et al.*²³

For proton scattering on ^{33}S up to $E_p = 4$ MeV, the only significant particle decay channels are p_0 , p_1 , and p_2 . The neutron channel is closed and no alpha particles were observed. [The $^{33}\text{S}(p, \alpha_0)^{30}\text{P}$ reaction has a Q value of -1.517 MeV; the resulting low-energy alpha particles

have very low penetrabilities.] The energies, spins, and parities of the final states in ^{33}S are ground state, $\frac{3}{2}^+$; $E_1 = 0.840$ MeV, $\frac{1}{2}^+$; and $E_2 = 1.987$ MeV, $\frac{5}{2}^+$. Our choice for the angular momentum coupling scheme is the channel spin representation. The intrinsic spins of the target nucleus I and the projectile i are coupled to form a channel spin s ($I+i=s$). The channel spin s and the orbital angular momentum l are coupled to form the total angular momentum J of the intermediate state ($s+l=J$). In the exit channel, the coupling is $s'+l'=J$ and $C+i=s'$, where C is the final-state spin and s' the exit channel spin. For proton scattering on nonzero spin targets, the compound states generally have several formation and decay channels. A channel is specified by the particle pair, spin J , channel spin s , orbital angular momentum l , and a partial reduced width amplitude γ . States may decay with two orbital angular momenta (l mixing and/or two channel spins (s mixing)). The angular distributions of the reaction products depend on these mixtures.

Because the targets were not isotopically pure, the excitation functions contained resonances due to the 11% ^{32}S contaminant. Fortunately the $^{32}\text{S}(p,p)^{32}\text{S}$ reaction has been well studied and the level density is small enough to allow correction of the measured excitation functions for the ^{32}S contribution. We used an iterative procedure to remove the ^{32}S yield from the yield curves. First the excitation functions were fit neglecting the ^{32}S contaminant. Then ^{32}S excitation functions were generated using the known ^{32}S resonance parameters²⁴ as a guide and combined (using the appropriate isotopic ratio) with the preliminary calculation for the ^{33}S excitation function. This combined excitation function was compared with the experimental yield curve, and a new set of ^{33}S resonance parameters obtained. Two iterations were usually sufficient to extract reliable ^{33}S resonance parameters up to $E_p \approx 3.4$ MeV. The resulting differential cross section for proton elastic scattering at 165° is shown in Figs. 1 and 2. Usually the subtraction of the calculated yield for the $^{32}\text{S}(p,p)^{32}\text{S}$ reaction from the measured cross section did not reduce the quality of the data. Difficulties did occur at energies where ^{33}S resonances overlapped resonances of similar size from the ^{32}S contaminant. This problem was particularly severe for the resonances near $E_p = 1.9$ and 3.1 MeV.

There are essentially no other elastic scattering resonance measurements for ^{33}S . Dassie *et al.*¹¹ studied four resonances at $E_p = 1.057$, 1.545, 1.742, and 1.997 MeV, which had been observed in the (p, γ) reaction. The first resonance is below the energy range of the present experiment and the next two resonances are weak $l=3$ resonances, which we did not observe. The 1.997-MeV resonance is discussed in Sec. IV. van der Leun and Endt²⁵ measured the $^{33}\text{S}(p, p'\gamma)^{33}\text{S}$ reaction in the energy range $E_p = 1.2\text{--}3.2$ MeV and identified 44 resonances from the deexcitation γ rays. The $(p, p'\gamma)$ experiment is much more sensitive to weak resonances than is the present (p, p') experiment.

Unique spins and partial widths were normally obtained for s - and p -wave resonances. The laboratory

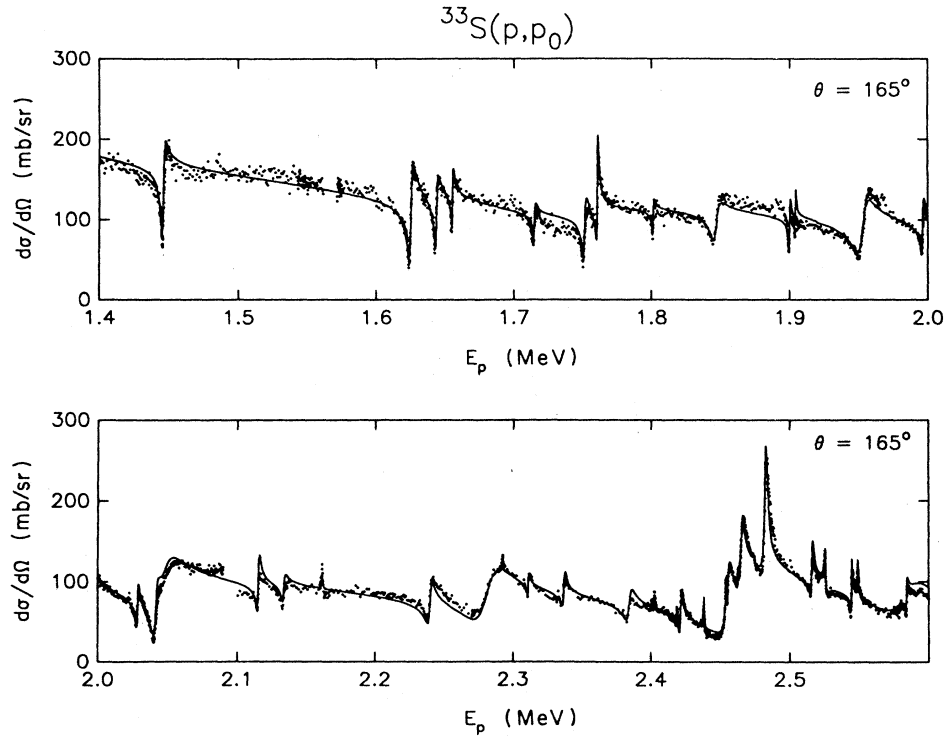


FIG. 1. Differential cross section for $^{33}\text{S}(p,p_0)^{33}\text{S}$ at 165° in the energy range $E_p = 1.4$ – 2.0 MeV (upper) and $E_p = 2.0$ – 2.6 MeV (lower). The solid line is an R -matrix fit.

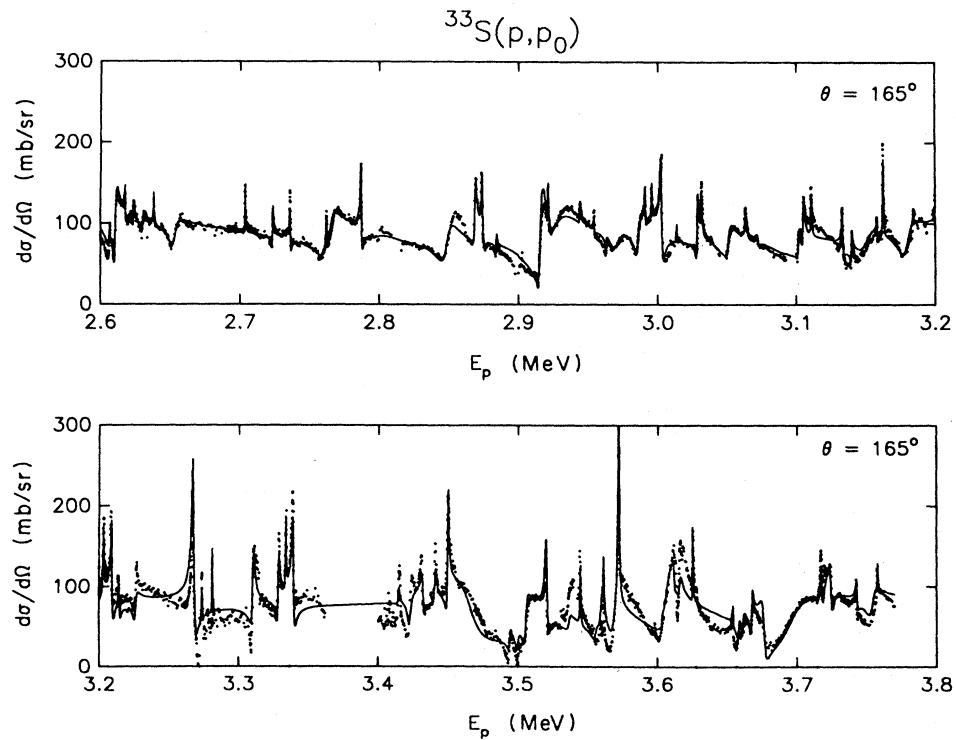


FIG. 2. Differential cross section for $^{33}\text{S}(p,p_0)^{33}\text{S}$ at 165° in the energy range $E_p = 2.6$ – 3.2 MeV (upper) and $E_p = 3.2$ – 3.8 MeV (lower). The solid line is an R -matrix fit.

widths for s - and p -wave resonances are much larger than the experimental resolution and channel spin interference effects are observed for many resonances. Definite solutions were not usually obtained for the weaker d - and f -wave resonances.

Channel spin mixing ratios are often difficult to determine well.²³ However, in the present data, there are regions where the channel spin is rather well determined because of interference between neighboring resonances. Particularly in the energy range $E_p \approx 1.8$ – 2.6 MeV, the interlevel interference clearly identifies the dominant channel spin. It is interesting to note that the dominant channel spin is often better determined than is the J value for $l=2$ and $l=3$ resonances.

The angular distributions for the (p, p_1) and (p, p_2) reactions do not provide sufficient information to extract precise mixing ratios for the inelastic channels. However, in many cases the dominant channel spin for the inelastic channel can be determined once the entrance channel mixing is obtained.

States with spin and parity 0^- are very difficult to identify. These states have a shape characteristic of p -wave resonances, but with a very small vertical excursion (from the Coulomb cross section). The size of a 0^- resonance is often comparable to the yield changes observed as the beam spot moves slightly on the target. Therefore 0^- states must be identified by repeated measurements. Two 0^- states may have been observed in the present experiment. The first occurs at $E_p = 1.375$ MeV. A small p -wave resonance shape was observed in several experimental runs. The excursion in the cross section was too small for a 1^- state with only an elastic scattering amplitude. Inelastic channels reduce the peak elastic resonance cross section, but in the present experiment no inelastic scattering was observed for this resonance. In the more sensitive $(p, p'\gamma)$ experiment by van der Leun and Endt,²⁶ no state was observed at this energy. This possible 0^- state would have a width of 8 ± 2 keV, with a corresponding reduced width of 700 keV. Such an extremely large reduced width makes the existence of this state very unlikely. A second possible 0^- state was tentatively identified at $E_p = 3.2240$ MeV; its reduced width is small.

The resonance parameters are reliable up to $E_p \approx 3.4$ MeV. Typical uncertainties are $\pm 10\%$ for laboratory widths a few keV or smaller and $\pm 20\%$ for large widths (tens of keV). Above $E_p \approx 3.4$ MeV, the quality of the fits deteriorates due to the complexity of the data. The resonance parameters obtained in this region are tentative. Only the resonances below $E_p = 3.25$ MeV are included in the detailed analysis presented below. The resonance parameters are listed in Table I.

IV. RESULTS

A. Level density

These data should provide the best available information on ^{34}Cl levels between 6.3- and 8.8-MeV excitation energy. The levels of ^{34}Cl with known parities (approximately 230, including 120 new levels obtained in the present experiment) are shown in Fig. 3. In general, information is extremely difficult to obtain for levels in a re-

gion above the low-lying bound levels [the levels observed as final states in the (p, γ) reaction and in most transfer reactions] and below the unbound levels observed in elastic scattering. Since for ^{34}Cl the proton separation energy is only 5.14 MeV, this typical blank region may be smaller than usual or even nonexistent. In the simplest constant temperature model, the nuclear level density is expected to increase as $\exp(E_x/T)$, where E_x is the excitation energy and T is the nuclear temperature. A plot of the cumulative number of levels up to an energy E_x is shown in Fig. 4. This plot shows the overall behavior of the level density, and emphasizes the regions with a larger fraction of missing levels. The level density generally agrees with the expected exponential increase; a nuclear temperature of $T = 2.1$ MeV is obtained from the data. There are two regions which seem anomalous. In the region $E_x = 5.0$ – 5.5 MeV there are few levels observed; this indicates levels missing just below the proton separation energy. There is also an interesting change in slope in the energy region $E_x = 6.9$ – 7.5 MeV (corresponding to $E_p = 1.8$ – 2.5 MeV). The energy region below $E_x = 7.1$ MeV ($E_p = 2.0$ MeV) has been measured by both the (p, γ) and (p, p) reactions, while the higher-energy region has been studied only with the (p, p) reaction. However, we believe that the apparent change in level density is not just a reflection of the change in the sensitivity of the two experimental methods. To investigate these and other questions, one must consider the strengths of the levels.

B. Strengths

Transforming from laboratory to reduced widths, $\gamma^2 = \Gamma/2P$ removes the kinematic effects due to the rapidly changing Coulomb penetrabilities. Reduced widths, cumulative reduced widths, and level positions are plotted versus incident proton energy in Figs. 5 and 6. Results are shown for each l, J^π combination with more than a few resonances. For those l, J^π combinations with channel spin mixing, the reduced widths have been summed over channel spin. These plots emphasize the strongest levels and any nonstatistical behavior in the strength distribution. It is striking that the average $l=1$ reduced width is more than 10 times larger than the average $l=0$ reduced width. There are a number of very strong $l=1$ levels: The 2^- states at 1.21 and 1.26 MeV have particularly large reduced widths of 320 and 240 keV. The negative- and positive-parity strengths are plotted in Fig. 7. Very little positive-parity strength is observed below $E_p = 2.4$ MeV, while the negative-parity strength decreases rapidly above $E_p = 2.6$ MeV. These effects are not kinematic. The s -wave resonances should be observed easily at the lower energies, while at the higher energies even weak p -wave resonances should be observed. The apparent change in level density in Fig. 4 is presumably a reflection of this localization of s - and p -wave strengths.

C. Analog states

The $T=1$ states in ^{34}Cl can be compared with states in ^{34}S and ^{34}Ar . The nucleus ^{34}Cl is unusual in that al-

TABLE I. Resonance parameters for $^{33}\text{S}(p,p)$. Unless otherwise noted, the entries are for the elastic (p_0) channel. The allowed channel spins are $s = s' = 1$ and 2 for p_0 , $s' = 0$ and 1 for p_1 , and $s' = 2$ and 3 for p_2 . An asterisk in the channel spin column indicates that any value of s fits equally well. Laboratory energies are quoted. See text for discussion of uncertainties in resonance energies, widths, and mixing ratios. The conventions for listing multiple solutions are (1) if several solutions give equivalent fits, then the solutions are listed in order of increasing J , and (2) if there is a strongly preferred solution it is listed first, with other solutions listed in parentheses.

E_p (MeV)	J^π	s	l	Γ (keV)	γ^2 (keV)	E_p (MeV)	J^π	s	l	Γ (keV)	γ^2 (keV)
1.214	2^-	1	1	1.6	320.0	2.4638	1^-	1	3	0.12	24.0
1.2633	2^-	1	1	0.8	120.0		2^-	*	3	0.07	14.0
		2	1	0.8	120.0		3^-	*	3	0.05	10.0
1.4448	2^-	1	1	1.0	64.0		4^-	*	3	0.04	8.1
		2	1	1.0	64.0		5^-	2	3	0.03	6.1
1.6245	3^-	2	1	3.0	95.0	2.4663	2^-	1	1	0.80	3.2
1.6430	2^-	1	1	1.0	30.0			2	1	2.8	11.0
		2	1	1.0	30.0	2.4763	1^+	1	2	0.15	2.91
1.6548	2^-	*	1	0.80	23.0	2.4838	2^+	2	0	2.5	4.7
1.7147	1^-	2	1	1.0	25.0	2.5173	1^+	1	0	1.2	2.2
1.7515	2^-	1	1	1.0	21.0			1	2	0.2	3.6
		2	1	1.0	21.0	2.5272	2^+	2	0	0.10	0.18
1.7608	2^+	2	0	0.80	6.1			1	2	0.40	7.1
1.8010	1^-	*	1	0.85	15.0			2	2	0.20	3.5
1.8464	1^-	2	1	5.0	80.0	2.5460	2^+	2	0	0.30	0.52
1.9000	1^-	2	1	0.6	8.2	2.5505	(1) $^-$	2	3	0.50	82.0
1.9046	1^+	1	0	0.15	0.79	2.582	1^-	2	1	32.0	110.0
		1	2	0.07	5.9	2.5856	2^-	1	1	0.70	2.4
1.9525	2^-	1	1	1.2	14.0		(1) $^-$	1	1	1.4	4.8
		2	1	6.8	81.0	2.6077	1^-	1	1	1.85	6.1
1.9964	2^-	1	1	1.35	14.0			2	1	0.15	0.50
		2	1	0.15	1.6	2.6085	1^+	2	2	0.16	2.4
	(3) $^-$	2	1	1.0	11.0		2^+	2	2	0.10	1.5
2.0286	2^-	1	1	0.2	2.0		3^+	2	2	0.07	1.1
		2	1	1.0	9.9		4^+	2	2	0.05	0.76
2.0416	2^-	1	1	3.0	29.0	2.6122	3^-	2	1	2.0	6.6
		2	1	1.0	9.6	2.6192	2^+	1	2	0.14	2.1
2.048	2^-	2	1	15.0	140.0		3^+	1	2	0.10	1.5
2.1157	2^-	1	1	1.6	13.0	2.6252	1^+	1	0	0.20	0.31
2.1338	1^-	1	1	1.5	12.0			*	2	0.10	1.5
		2	1	0.5	3.9		(2) $^+$	2	0	0.12	0.19
2.1621	1^+	1	0	0.15	0.46			*	2	0.06	0.9
		1	2	0.40	16.0	2.6317	1^-	1	1	1.3	4.2
2.2403	2^-	1	1	2.9	18.0	2.6397	1^-	2	3	0.15	20.0
		2	1	0.6	3.7		2^-	*	3	0.09	12.0
2.283	2^-	1	1	20.0	110.0		3^-	*	3	0.06	8.0
2.2932	1^-	2	3	0.10	32.0		4^-	*	3	0.05	6.6
	2^-	2	3	0.06	20.0		5^-	2	3	0.04	5.3
	3^-	2	3	0.04	13.0	2.6548	1^-	1	1	4.0	12.0
2.3120	2^-	2	1	0.70	3.8			2	1	2.0	6.2
2.3381	1^-	1	1	1.5	7.8	2.6984	0^+	2	2	0.27	3.5
		2	3	0.40	110.0		1^+	*	2	0.09	1.2
	2^-	1	1	0.90	4.7		2^+	*	2	0.05	0.69
		*	3	0.15	42.0	2.7055	1^-	2	3	0.23	26.0
2.3851	1^-	1	1	4.0	19.0		2^-	*	3	0.14	16.0
2.4034	2^+	2	0	0.1	0.21		3^-	*	3	0.10	12.0
		2	2	0.07	1.6	2.7252	1^+	1	0	0.30	0.42
2.4199	2^-	2	3	0.1	23.0		2^+	2	0	0.18	0.25
2.4225	2^-	1	1	1.2	5.3	2.7379	3^+	*	2	0.20	2.4
		1	3	0.2	45.0		4^+	2	2	0.15	1.8
2.4393	1^+	2	2	0.3	6.4	2.7641	3^+	2	2	0.04	0.46
2.4553	1^+	1	0	2.0	3.9		(1) $^+$	2	2	0.09	1.0
	2^+	2	0	2.0	3.9		(2) $^+$	2	2	0.06	0.64
2.4568	1^+	1	0	3.0	5.8	2.7661	2^-	1	1	10.0	27.0
2.461	3^-	2	1	40.0	170.0	2.7891	3^+	2	2	0.64	7.0

TABLE I. (Continued).

E_p (MeV)	J^π	s	l	Γ (keV)	γ^2 (keV)	E_p (MeV)	J^π	s	l	Γ (keV)	γ^2 (keV)
2.8510	4 ⁺	2	2	0.5	5.5	3.1426	2 ⁺	2	0	0.30	0.28
2.8508	2 ⁻	2	1	8.0	19.0	p_1	1 ⁻	1	2	0.20	6.1
2.8711	2 ⁺	2	0	1.2	1.4	3.1541	(3) ⁺	*	2	0.20	1.2
2.8763	3 ⁺	1	2	0.20	2.6	3.1611	3 ⁻	1	3	0.15	7.0
2.8866	1 ⁺	*	2	0.50	4.7	3.1656	2 ⁻	2	3	0.15	7.0
	2 ⁺	*	2	0.15	1.4	3.1832	p_1	1	1	6.0	9.9
	3 ⁺	*	2	0.09	0.84	3.1877	2 ⁺	2	0	4.0	22.0
	4 ⁺	2	2	0.06	0.59		*	2		0.30	0.27
2.9109	1 ⁺	2	2	0.05	0.46	p_1	0	2	0.15	4.2	3.0
2.9185	2 ⁺	2	0	0.20	1.8	3.2032	(2 ⁺)	2	2	0.10	0.5
2.9209	1 ⁺	1	0	3.0	3.5	3.2062	2 ⁻	2	3	0.40	17.0
		1	2	2.0	2.3		3 ⁻	2	3	0.30	13.0
2.9238	3 ⁺	1	2	0.7	6.2	3.2123	4 ⁺	2	2	0.80	4.6
2.9290	2 ⁻	1	1	0.3	2.6	3.2178	2 ⁺	*	2	0.40	2.3
	p_1	1	1	17.0	37.0		3 ⁺	*	2	0.29	1.7
2.9468	1 ⁺	1	0	2.0	18.0	(3.2240)	0 ⁻	1	1	0.30	0.47
		*	2	0.2	0.22	3.2293	2 ⁻	*	1	2.2	3.5
	2 ⁺	2	0	0.1	0.85	3.2704	4 ⁺	2	2	2.0	11.0
		*	2	0.12	0.13	3.2714	1 ⁺	*	2	2.5	13.0
2.9570	1 ⁺	*	2	0.06	0.5		2 ⁺	*	2	1.5	8.0
	2 ⁺	*	2	0.16	1.3	3.2769	1 ⁻	2	3	0.25	9.6
	3 ⁺	*	2	0.10	0.83		2 ⁻	*	3	0.15	5.8
	4 ⁺	2	2	0.07	0.58		3 ⁻	*	3	0.11	4.1
2.9656	2 ⁻	1	1	0.05	0.45		4 ⁻	*	3	0.08	3.2
		*	3	1.0	1.0		5 ⁻	2	3	0.07	2.6
2.9726	1 ⁻	2	1	0.10	0.83	3.2844	1 ⁻	2	3	0.23	8.9
	p_1	1	1	5.0	10.0		2 ⁻	*	3	0.14	5.3
2.9886	2 ⁻	2	1	3.0	25.0		3 ⁻	*	3	0.10	3.8
	p_1	1	1	4.0	8.1		4 ⁻	*	3	0.08	3.0
2.9937	2 ⁺	1	2	0.50	4.0		5 ⁻	2	3	0.06	2.4
	(1) ⁺	1	2	0.20	1.6	3.3135	2 ⁺	2	0	1.5	1.3
2.9982	1 ⁻	2	3	0.40	3.2	3.3318	2 ⁺	2	0	0.80	0.66
3.0052	3 ⁺	*	2	0.30	19.0	3.3371	(2) ⁻	*	3	0.30	11.0
	(2) ⁺	*	2	1.2	9.3	3.3424	3 ⁺	*	2	1.5	7.6
	(4) ⁺	2	2	1.7	13.0		4 ⁺	2	2	1.2	5.9
3.0162	1 ⁻	2	3	0.90	7.2	3.4186	1 ⁺	1	0	0.4	0.31
	2 ⁻	*	3	0.10	6.1		1 ⁻	1	2	0.4	1.8
	3 ⁻	*	3	0.06	3.7	3.4266	2 ⁻	*	1	2.0	2.6
	4 ⁻	*	3	0.04	2.6		p_2	2	1	0.80	63.0
	5 ⁻	2	3	0.03	2.0	3.4359	(2) ⁺	*	2	1.4	6.1
3.0313	2 ⁺	2	0	0.027	1.6		p_1	*	2	0.20	3.3
3.0343	1 ⁻	2	3	0.70	0.73		p_2	2	0	0.30	7.6
3.0538	(2) ⁻	1	1	0.50	30.0	3.4449	1 ⁻	2	3	1.0	30.0
3.0664	2 ⁺	2	0	5.0	9.4		p_2	2	1	0.40	29.0
		2	2	0.6	0.61	3.4534	2 ⁺	2	0	1.0	0.76
3.0754	0 ⁺	2	2	0.5	3.5		p_1	2	2	0.50	2.1
3.0979	2 ⁻	1	1	1.0	7.0	3.4539	2 ⁻	2	3	0.45	13.1
		2	1	3.0	5.4	3.469	2 ⁺	2	2	25.0	110.0
	p_1	1	1	20.0	130.0	3.4981	3 ⁻	2	1	1.0	1.2
3.1045	1 ⁻	1	1	1.2	2.1		p_2	2	1	1.0	58.0
3.1080	1 ⁺	1	0	0.90	0.88	3.5041	3 ⁻	2	1	1.0	1.2
3.1138	1 ⁻	2	3	0.50	26.0		p_2	2	1	1.0	57.0
	2 ⁻	*	3	0.30	15.0	3.509	1 ⁺	1	0	10.0	7.3
3.1362	3 ⁺	*	2	0.50	3.2		p_1	1	0	15.0	23.0
		*	4	0.10	3.1	3.5101	2 ⁻	1	1	3.0	3.7
	p_1	2	1	0.40	2.6	3.5247	4 ⁺	2	2	1.5	5.9
	p_1	*	4	0.10	3.0	3.5412	1 ⁺	1	0	1.0	0.72

TABLE I. (Continued).

E_p (MeV)	J^π	s	l	Γ (keV)	γ^2 (keV)	E_p (MeV)	J^π	s	l	Γ (keV)	γ^2 (keV)
		1	2	0.60	2.3	3.6586	1^+	2	2	0.50	1.7
3.5492	p_1	1	2	1.5	20.0	3.6626	2^+	2	0	1.0	0.67
		4 $^-$	1	3	0.20			0	2	0.50	5.4
3.5603	p_2	3	1	0.20	9.4	3.6656	1^-	1	1	1.5	1.6
		1 $^+$	1	0	1.0	3.6721	1^+	1	0	0.80	0.53
3.5643	p_1	1	2	2.0	26.0	3.6806	3^+	1	2	3.0	9.9
		2 $^+$	2	0	3.0			1	2	1.0	11.0
3.5658		3 $^-$	2	3	0.20	3.6997	3^-	2	1	35.0	37.0
3.5733		3 $^-$	2	1	5.0	3.7218	1^-	2	3	0.70	14.0
3.5763	p_1	*	3	1.0	120.0	3.7238	1^-	2	1	2.0	2.1
		4 $^-$	*	3	0.70			2	1	2.0	51.0
		5 $^-$	2	3	0.60	3.7288	3^+	1	2	0.80	2.5
3.6074		1 $^-$	2	1	0.30			2	2	0.20	0.63
	p_2	2	1	0.30	11.0			1	2	0.20	1.9
3.6114		2 $^+$	2	0	10.0			3	0	0.40	3.6
3.6159	(1) $^+$	1	2	1.0	3.6	3.7473	3^+	1	2	0.40	1.2
3.6199	(1) $^+$	1	0	1.0	0.69			1	2	0.10	0.9
3.6295	p_2	2	2	0.80	210.0			3	0	0.30	2.6
		4 $^-$	*	3	0.18	3.7589	2^-	1	1	6.0	6.1
		5 $^-$	2	3	0.15	3.7624	1^-	2	3	0.2	3.7

though the third component of isospin [$T_3 = (N - Z)/2$] is zero, the ground state has $T = 1$. The analog states observed by proton resonances have parent states which are at low excitation energy in ^{34}S . Spectroscopic information on states in ^{34}S has been obtained with the $^{33}\text{S}(d,p)^{34}\text{S}$ reaction by van der Baan and Sikora²⁶ for $E_x(^{34}\text{S}) < 6.6$ MeV and by Crozier²⁷ for $E_x(^{34}\text{S}) < 8.2$ MeV. The spectroscopic factors of van der Baan are consistently smaller than those of Crozier (see tabulation in Ref. 3). Some information is available on the location and angular momentum of states in ^{34}Ar from the $^{36}\text{Ar}(p,t)^{34}\text{Ar}$ reaction.⁶

Much of the existing information on analog states comes from proton capture studies and is summarized by Waanders *et al.*⁸ The $^{33}\text{S}(^3\text{He},d)^{34}\text{Cl}$ experiment by Erskine *et al.*⁵ provides proton spectroscopic factors for those states at $E_x(^{34}\text{Cl}) < 4.6$ MeV. Although γ -ray branchings and strengths have provided much information on the isospin character of states in ^{34}Cl , definitive identification of the corresponding analog and parent states has proved difficult in the energy range $E_x > 4.1$ MeV.

Analog states observed in proton elastic scattering studies are identified by comparison of excitation energies and of neutron and proton spectroscopic factors,²⁸ with $S_{dp} = S_n$ and $S_p = (2T + 1)\Gamma_p/\Gamma_{sp}$. The proton single-particle widths Γ_{sp} for the analog states were calculated with the method of Zaidi and Darmodjo²⁹ and Harney³⁰ as described by Harney and Weidenmüller.³¹ The variation in single-particle widths due to the uncertainties in optical-model parameters is estimated to be about 15%.³² In order to compare directly with the (d,p) data, the optical-model potential well parameters were taken from the (d,p) analysis.²⁷ Of the states in ^{34}S which are populated in the neutron transfer reaction and whose analogs

should occur in the range of the present experiment, most have spectroscopic factors large enough that the analogs should be observed in elastic scattering. Results for 10 analog candidates are listed in Table II and discussed below. For many of the parent states, the spin assignments are uncertain, which makes the analog identification tentative. The neutron spectroscopic factors listed are those of Crozier, while the excitation energies and spins are from Endt.⁴ Individual states are discussed below.

The $E_x(^{34}\text{S}) = 6.479$ -MeV state. The (d,p) spectroscopic factor of the $(1-3)^-$, $E_x(^{34}\text{S}) = 6.479$ -MeV state was characterized by Crozier²⁷ as $l = 1$ with $(2J + 1)S_n = 3.6$; van der Baan and Sikora²⁶ obtained a spectroscopic factor of $(2J + 1)S_n = 1.2$, and commented that the observed proton group in the (d,p) reaction has complex structure. Endt⁴ assigns $(1,2)^-$ for the 6.479-MeV state in ^{34}S . The proton capture experiments of Waanders *et al.*⁸ restricted the possible spin assignments for this resonance to $3^+(2)$. The only strong proton resonance which seems a reasonable candidate to be the analog is the 2^- state at $E_p = 1.4448$ MeV, which has strength $(2J + 1)S_p = 1.8$. The nearest 1^- candidates are about 200 keV away.

The $E_x(^{34}\text{S}) = 6.685$ -MeV state. Neutron transfer to the $(0-3)^-$, $E_x(^{34}\text{S}) = 6.685$ -MeV state has been characterized by Crozier as $l = 1$ with $(2J + 1)S_n = 1.3$. According to Endt,⁴ the γ decay of this state suggests that a $J = 3$ assignment is very improbable. The analog of this state is expected to lie near $E_p = 1.63$ MeV. The states at 1.6430 and 1.6548 MeV are candidates to be the analog of this parent state. Although Waanders *et al.* tentatively identified the state at $E_p = 1.6430$ MeV as $T = 0$, the γ decay does not exclude $T = 1$ for this state. Since the two resonances have the same J^π and are close in energy, the

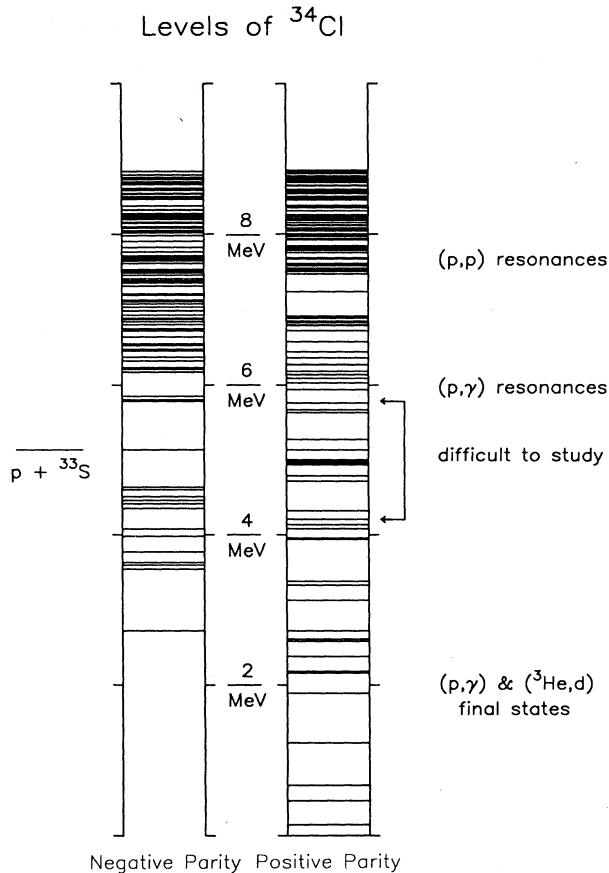


FIG. 3. Levels of ^{34}Cl from the ground state to 8 MeV. Approximately 120 of the total of 230 levels were first observed in the present experiment.

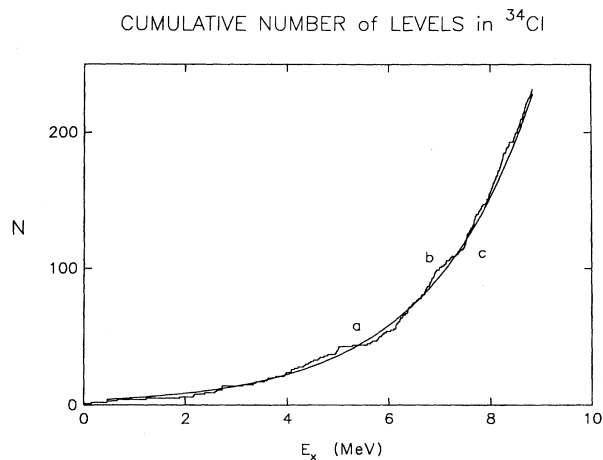


FIG. 4. Cumulative number of levels observed in ^{34}Cl as a function of excitation energy. The flat region labeled "a" indicates levels missing at energies just below the proton separation energy. The change in slope at point "b" may indicate a decrease in sensitivity to small resonances in the proton elastic scattering experiments as compared with the proton capture experiments. The increase in slope at point "c" corresponds to the onset of s -wave resonances at energies $E_p > 2.4$ MeV. See text for discussion.

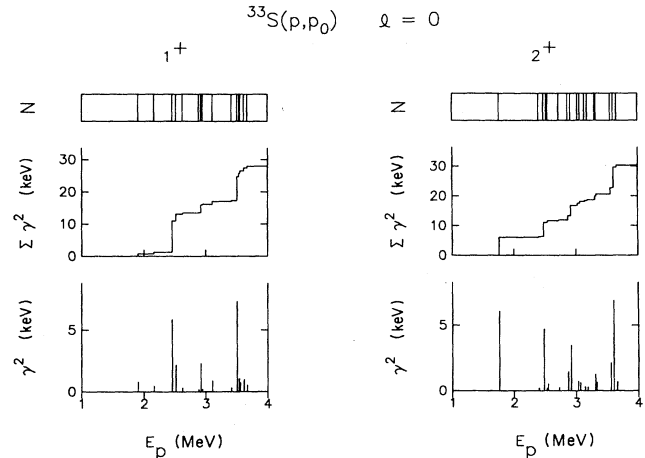


FIG. 5. Proton reduced widths and cumulative sum of reduced widths vs energy for $l=0$ resonances in $^{33}\text{S}(p,p_0)^{33}\text{S}$. Reduced widths are typically less than a few keV. The resonance locations are shown at the top of the figure.

analog strength is presumably shared. Both states are listed in Table II.

The (d,p) transfer to the $J=2$ state at $E_x(^{34}\text{S})=6.829$ MeV was determined by Crozier to be $l_n=0$, with $(2J+1)S_n=0.56$. This state was assigned $J^\pi=2^+$ by Endt on the basis of (t,p) data.³³ The resonance at $E_p=1.7512$ MeV was assigned as the analog of this parent state by Endt and van der Leun³ on the grounds (1) that the state decays to one or more $T=0$ states with a strength exceeding the recommended upper limit³⁴ for isoscalar $E1$ or $M1$ transitions and (2) that the spectroscopic factor for stripping agrees with that for the parent state in ^{34}S . Dassie *et al.*¹⁰ assigned the $E_p=1.752$ -MeV resonance $J=(1^+,2)$, while Waanders *et al.* assigned $J=2; T=1$. The present data indicate that the resonance is definitely p wave. Therefore $J^\pi=2^-$; the proton spectroscopic factor is $(2J+1)S_p=0.60$. The only nearby positive-parity resonance is at $E_p=1.761$ MeV, which has $J=2^+$, but a much smaller strength $(2J+1)S_p=0.10$. The next nearest positive-parity state is at $E_p=1.90$ MeV, but this state is also weak. The origin of the disagreement is unknown.

The $E_x(^{34}\text{S})=6.954$ -MeV state has been assigned $J^\pi=(0-3)^-$, with $(2J+1)S_n=0.84$ by Crozier. Endt and van der Leun assigned this state $J^\pi=2^-$, with the J value based on an $(\alpha,p\gamma)$ experiment. The resonances at $E_p=1.8464$ and 1.9525 MeV are candidates to be the analog of this level. Our results indicate that the resonance at $E_p=1.8464$ MeV has $J^\pi=1^-$ and the resonance at $E_p=1.9525$ MeV has $J^\pi=2^-$. On the basis of the present spin assignments, the resonance at $E_p=1.9525$ MeV is the analog with a strength of $(2J+1)S_p=1.5$.

The $E_x(^{34}\text{S})=7.110$ -MeV state was observed by Crozier to have significant $l=1$ and $l=3$ components: $(2J+1)S_n=0.52, 1.76$, and $J=(3)^-$. Endt and van der Leun assigned $J^\pi=2^-$ as determined from $(\alpha,p\gamma)$ experiments. Endt's more recent compilation⁴ lists a 3^- assign-

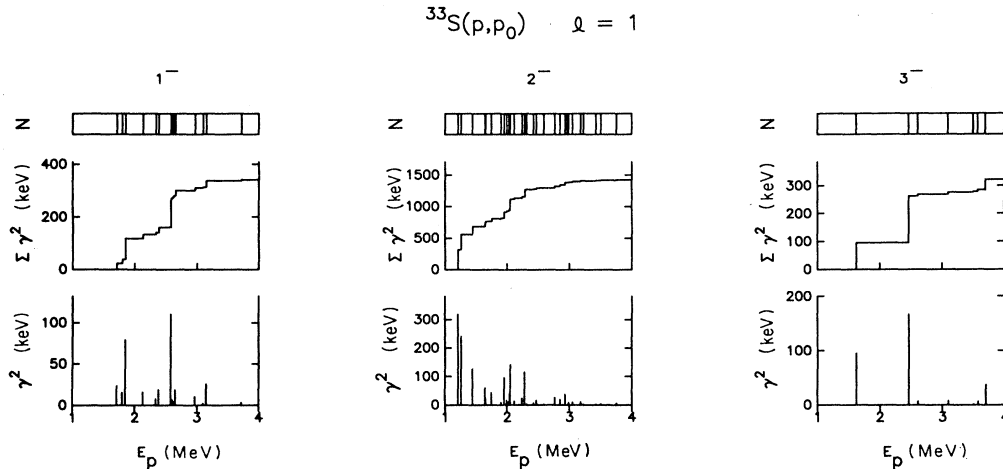


FIG. 6. Proton reduced widths and cumulative sum of reduced widths vs energy for $l=1$ resonances in $^{33}\text{S}(p,p_0)^{33}\text{S}$. Reduced widths are typically tens of keV. The resonance locations are shown at the top of the figure.

ment. A candidate to be the analog of this state is the resonance at $E_p = 1.9964$ MeV, which has been assigned $T=1$ by Waanders *et al.* Due to the low penetrability, the f -wave component corresponds to an $l=3$ laboratory width which is unobservable as compared with the large $l=1$ laboratory width. The elastic scattering data of Dassie *et al.*¹¹ indicated $J^\pi = 2^-$ or 3^- . Based on the recommended upper limits for γ -ray transition strengths, Dassie assigned $J=3$ to the resonance. However, the present data favor the $J=2$ assignment. Our analysis indicates that the p -wave spectroscopic factor for this resonance is $(2J+1)S_p \approx 0.23$ for either $J=2$ or 3 .

Identification of the analog states discussed above was assisted by information from the (p,γ) reaction. There is no proton capture data for resonances lying above $E_p = 2$ MeV. For this reason the analog identification in this region is guided by three ^{34}S states with large spectroscopic factors [$E_x(^{34}\text{S}) = 7.630, 7.781, \text{ and } 8.138$ MeV]. These analogs should be the most easily identified in the proton excitation function and are considered first.

The 3^- state at $E_x(^{34}\text{S}) = 7.630$ MeV has a very large spectroscopic factor of $(2J+1)S_n = 3.92$. The analog is clearly the $E_p = 2.46$ MeV, 3^- resonance with $(2J+1)S_p = 3.5$.

The 1^- resonance at $E_p = 2.58$ MeV is probably the analog of the $E_x(^{34}\text{S}) = 7.781$ -MeV state. The p -wave neutron spectroscopic factor for the parent state is $(2J+1)S_n = 1.08$, while the spectroscopic factor for the analog resonance is $(2J+1)S_p = 0.99$.

The $E_x(^{34}\text{S}) = 8.138$ -MeV state was assigned $J^\pi = (0-3)^-$ with $(2J+1)S_n = 1.04$ by Crozier. Endt⁴ assigns the spin and parity as 1^- . The resonance at $E_p = 2.9290$ MeV is fit best with spin 2 (there is strong interference with neighboring resonances). Based on energy considerations this state is a good candidate to be the analog of the 8.138-MeV excited state in ^{34}S . The proton spectroscopic factor is $(2J+1)S_p = 0.58$ —this is smaller than the parent state spectroscopic factor. There seems to be no other reasonable choice for the analog which has sufficient strength: As noted above, there is very little $l=1$ strength above the strong resonance at $E_p = 2.58$ MeV.

The state at $E_x(^{34}\text{S}) = 7.653$ MeV is populated entirely by $l=3$ neutron transfer with $(2J+1)S_n = 2.28$. Endt⁴ does not list a spin for this state. Crozier assigned $J^\pi = (3,4)^-$, but gave no reason for the assignment. The only candidate to be the analog of this state with comparable strength is the $E_p = 2.550$ MeV, $1^-(2,3)^-$ resonance with $(2J+1)S_p = 0.96$. The next nearest f -wave resonances are at 2.464 and 2.640 MeV with corresponding strengths of $(2J+1)S_p = 0.27$ and 0.25, respectively.

The state at $E_x(^{34}\text{S}) = 7.732$ MeV has been assigned spin $(2,3)^-$ with neutron transfer spectroscopic factors of $(2J+1)S_n = 0.12, 0.56$ by Crozier. This state was not listed in the 1978 Endt and van der Leun compilation.³ Endt⁴ lists this state as (0^+-3^+) . There are two negative-parity resonances which are candidates to be the analog of this state. The resonance at $E_p = 2.6085$ MeV has been assigned $J^\pi = 1^-$ with $(2J+1)S_p(l=1) = 0.06$. The resonance at $E_p = 2.6122$ MeV has been assigned $J^\pi = 3^-$

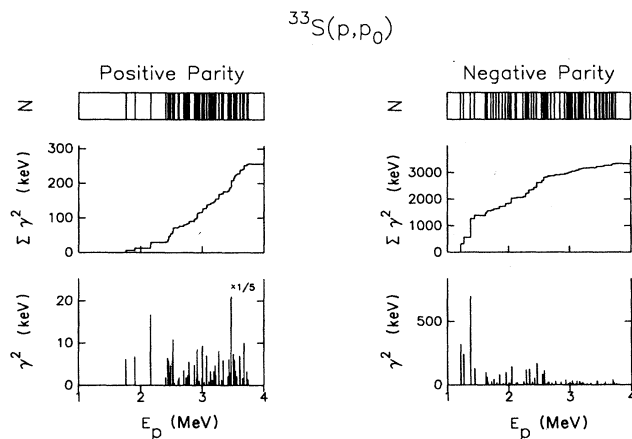


FIG. 7. Distribution of positive- and negative-parity strength in $^{33}\text{S}(p,p_0)^{33}\text{S}$. There is very little positive-parity strength below $E_p = 2.4$ MeV, and very little negative-parity strength above $E_p = 2.6$ MeV.

with $(2J+1)S_p(l=1)=0.14$. In both cases only the p -wave component is expected to be observed.

The energy order of the proposed analogs of the parent states at $E_x(^{34}\text{S})=7.732$ and 7.781 MeV are interchanged. Level crossings are not possible if the states have the same spin and parity. If the previous analog identifications and the 1^- assignment for the $E_p=2.58$ -MeV resonance are correct, then the state at $E_p=2.6122$ MeV seems the best choice to be the analog of $E_x(^{34}\text{S})=7.732$ MeV.

The state at $E_x(^{34}\text{S})=7.753$ MeV has been assigned $J^\pi=(0-3)^-$ with a p -wave neutron spectroscopic factor of $(2J+1)S_n=0.32$ by Crozier. The locations of the weaker analog resonances discussed above suggest that the resonance at $E_p=2.655$ MeV may be a suitable candidate. Only a tentative assignment is possible since the spin of the parent state is unknown.

The identification of analog states in ^{34}Cl is much more tentative than, for example, for analog states in neighboring nuclei² such as ^{32}S . This suggests that either the (d,p) results are not as reliable as usual, or that the spins of some levels in ^{34}S are in error. These difficulties in establishing the isospin character of the resonances are particularly important if one hopes to establish a complete level scheme for ^{34}Cl .

D. Sum rules

The simplest shell-model description of the nucleus ^{34}Cl is a proton and neutron coupled to a ^{32}S core. In this description the level scheme of ^{34}Cl contains much information on the two-body residual interaction in the $2s-1d$ shell.

Wildenthal *et al.*^{35,36} performed extensive shell-model calculations in the $A=30-35$ region and the $A=34-38$

region. These calculations for positive-parity states have been compared with the (d,p) results of van der Baan and Sikora²⁶ and the $(^3\text{He},d)$ results of Erskine *et al.*⁵ Calculations for negative-parity states have been performed by Ern e for the mass region $A=33-41$ using a $d_{3/2}f_{7/2}$ configuration.³⁷ Analysis of the states below ~ 7 MeV provided much information about major components of the $(d_{3/2})^2$ configuration and of the $d_{3/2}f_{7/2}$ $T=0$ and 1 configurations²⁷ in ^{34}S . Measurements by Erskine *et al.*⁵ allowed identification of the major components of the $(d_{3/2})^2$ and $d_{3/2}f_{7/2}$ $T=0$ and 1 configurations in ^{34}Cl .

Consider the summed strength in the present data. The single-particle reduced widths obtained from an R -matrix approach apply for a specific channel (s,l,J,π,T) . The single-particle reduced widths are estimated²⁸ by $\gamma_{\text{sp}}^2 = (\frac{5}{8})(h^2/ma^2)$ ($=940$ keV for $p+^{33}\text{S}$), where m is the reduced mass and the radius a is given by $a=r_0(1+A^{1/3})$, with $r_0=1.2$ fm. Below the Coulomb barrier, this simple estimate provides values which are consistent with those obtained in more sophisticated calculations for analog states. It is convenient to sum over some of the quantum numbers, particularly when the number of levels is small. The sum rule for N channels is obtained³⁸ by multiplying the single-particle reduced width by N . The summed strengths and number of levels are listed in Table III and the measured fraction of the sum rule is listed in Table IV for s - and p -wave resonances. The p - and f -wave strengths are much larger than the s - and d -wave strengths. There is very little positive-parity strength in this region of ^{34}Cl .

E. Strength functions

The strength function $S \equiv \langle \gamma^2 \rangle / D$ provides information on the strength of the average nucleon-nucleus po-

TABLE II. Analog resonances.

$^{34}\text{S}^a$				^{34}Cl				$E_x(\text{S}) - E_x(\text{Cl})$ (keV)	
J^π	E_x (MeV)	l_n	$\hat{J}^2 S_n$	J^π	l_p	E_x^b (MeV)	E_p (MeV)		
$(1,2)^-$	6.479	1	3.64	2^-	1	6.545	1.4448	1.8	-66
$(0-2)^-$	6.685	1	1.28	2^-	1	6.737	1.6430	0.88	-52
				2^-	1	6.749	1.6548	0.34	-64
2^+	6.829	0	0.56	2^-^c	1	6.842	1.7512	0.60	-11
2^-	6.954	1	0.84	2^-	1	7.038	1.9525	1.5	-84
3^-	7.110	1	0.52	$(2)^-^c$	1	7.080	1.9964	0.23	30
		3	1.76		3			d	
				$(3)^-$	1			0.22	
					3			d	
3^-	7.630	1	3.92	3^-	1	7.531	2.461	3.5	99
J^-	7.653	3	2.28	1^-	1	7.618	2.550	0.96	35
$(2,3)^-$	7.732	1	0.12	3^-	1	7.678	2.6122	0.14	54
		3	0.56		3			d	
1^-	7.781	1	1.08	1^-	1	7.649	2.582	0.99	132
1^-	8.138	1	1.04	2^-	1	7.985	2.9290	0.58	153

^a Excitation energies, spins, and parities are from Endt (Ref. 4). Spectroscopic factors are from Crozier (Ref. 27).

^b Assuming $S_p=5.1425$ MeV (Ref. 8).

^c See text for discussion.

^d The $l=3$ component is expected to be below the limit of observability.

TABLE III. Cumulative proton strength in ^{34}Cl .

J^π	l	$\sum \gamma^2$	$\sum \gamma^2$	$\sum \gamma^2$
		$T=0$ (keV)	$T=1$ (keV)	$T=0$ and 1 (keV)
1^+	0	17 (10) ^a	—(0)	17 (10)
2^+	0	19 (12)	—(0)	19 (12)
1^-	1^b	144 (10)	193 (3)	338 (13)
2^-	1^b	1195 (24)	222 (4)	1417 (28)
3^-	1	—(0)	269 (3)	269 (3)
all	0	36 (22)	—(0)	36 (22)
all	1^c	1339 (34)	684 (10)	2024 (44)

^aThe sums of reduced widths in the energy range $E_p = 1.20$ – 3.25 MeV are listed, with the corresponding number of levels in parentheses. A dash indicates that no levels were observed.

^bSummed over both channel spins.

^cThe 0^- states are omitted.

tential. Values of the strength function over a range of nuclei help determine the mass dependence of the optical-model potential well parameters. The existence of spin-orbit and spin-spin terms in the nuclear force will result in a difference in strength functions for different s , l , and J . Because many analog states have been identified, it also may be useful to separate the strength functions according to isospin. Because of the small sample size, most of the strength functions for specific channels are poorly determined. Values of the measured strength functions for the $l=0$ and 1 channels are listed in Table V. For individual channels the error quoted is $(2/N)^{1/2}$ —the fractional statistical error for a Porter-Thomas distribution. Channels not listed in Table V have too few states for meaningful analysis. The $l=2$ and 3 strength functions are not listed; due to the low penetrability a large fraction of the strength is not observed at the lower bombarding energies. Essentially all of the p -wave strength appears to be located at $E_p < 2.5$ MeV, with very little positive-parity strength in this region: the p -wave strength function in this energy region

TABLE IV. Fraction of the proton strength sum rule in ^{34}Cl .

J^π	l	$T=0$	$T=1$	$T=0$ and 1
		(%)	(%)	(%)
1^+	0	2		1
2^+	0	2		1
1^-	1^a	7	10	9
2^-	1^a	63	12	38
3^-	1		29	15
all	0	2		1
all	1^b	28	15	21

^aSummed over both channel spins.

^bThe 0^- states are omitted.

is 10–100 times larger than the s -wave strength function.

Most analyses of the p -wave strength functions obtained from average neutron capture cross sections in the keV region have employed the simplifying assumption that the p -wave strength function is independent of J . However, identification of p -wave resonances and their spins is much easier in proton elastic scattering, due to the strong l and J dependence of the characteristic resonance shapes. Strength functions for many of the individual channels have been determined from the present data. To obtain the strength function for a given l , the contributions from the individual channels must be averaged with the appropriate weighting factors. Lynn³⁸ suggests employing an averaging procedure

$$S(l) = \frac{2}{2(2l+1)} \sum_{s=|l-1/2|}^{l+1/2} \sum_J \frac{(2J+1)}{(2i+1)(2I+1)} S(sJl)$$

for the l -wave strength function. The strength functions for individual channels $\{sJl\}$ and the strength function for a given l are listed in Table V. In the present $l=0$ data the strength functions for the two channels are about equal. For the $l=1$ data, essentially no 0^- states are observed and only a few 3^- states are seen. Most of the strength is in the 2^- states. The major qualitative re-

TABLE V. Proton strength functions in ^{34}Cl .

s	l	J^π	T	N	$\sum \gamma^2$ (keV)	$\langle \gamma^2 \rangle / D$
1	0	1^+	0	10	17	0.013 (5) ^a
2	0	2^+	0	12	19	0.012 (5)
weighted average of $l=0$, $T=0$						
1	1	1^-	0	10	84	0.054 (24)
2	1	1^-	0	10	60	0.037 (17)
1	1	2^-	0	24	721	0.344 (99)
2	1	2^-	0	24	477	0.225 (66)
weighted average of $l=1$, $T=0$						
1	1	1^-	1	3	3	0.004 (3)
2	1	1^-	1	3	189	0.161 (66)
1	1	2^-	1	4	136	0.069 (49)
2	1	2^-	1	4	86	0.044 (31)
2	1	3^-	1	3	269	0.186 (152)
weighted average of $l=1$, $T=1$						
average of $l=1$, $T=0+1$						
						0.098 (46)
						0.113 (29)

^aQuantities in parentheses are the uncertainties in the last digit.

sult is that the $l=1$ strength function is more than an order of magnitude larger than the $l=0$ strength function.

The ratio of s -wave strength functions for channel spins 1 and 2 is $S_1/S_2=1.1\pm 0.7$. The large uncertainty in the s -wave strength function ratio is due to the extremely small sample sizes. Since p -wave scattering is particularly strong for this nucleus, it is tempting to look for possible splitting between the $p_{1/2}$ and $p_{3/2}$ strength functions. Most of the existing data on the angular momentum dependence of proton strength functions is obtained from experiments on zero spin targets.^{28,39} The $p_{1/2}$ proton size resonance was observed²⁸ to have a maximum near $A=42$. There is only fragmentary experimental evidence about the location of the $p_{3/2}$ size resonance. From the available data on zero spin targets, the $p_{3/2}$ strength function is several times smaller than the $p_{1/2}$ strength function over the mass range $A=40-60$. It would be interesting to examine the $p_{1/2}$ and $p_{3/2}$ strength functions in the present data, since the $p_{3/2}$ size resonance should be very close to $A=34$. However, the present analysis provides widths in the channel spin representation. This is the natural representation since channel spins are incoherent for unpolarized beams and targets. The transformation of reduced width amplitudes from the channel spin representation to the particle angular momentum representation is

$$\gamma_j = \sum (-)^{l+i-j} (2s+1)^{1/2} (2j+1)^{1/2} W(IiJl; sj) \gamma_{slj},$$

where W is a Racah coefficient. The signs of amplitudes are generally unknown. If the amplitudes are assumed to have random signs, the cross terms will cancel on the average and the reduced widths transform according to

$$\gamma_j^2 = \sum (2s+1)(2j+1) W^2(IiJl; sj) \gamma_{slj}^2.$$

Although one may expect to obtain approximate values for the strength functions in the j representation, the loss of sign information has a severe impact for small sample sizes. A Monte Carlo simulation was performed to estimate the error resulting from the neglect of cross terms. We considered N levels with $l=1, J=2$. For each level in the sample, the reduced width amplitudes $\gamma_{slj} = \gamma_{112}$ and γ_{212} were drawn from a Gaussian distribution of mean zero (corresponding to a Porter-Thomas distribution of reduced widths). The average $l=1, j=\frac{1}{2}$ strength was calculated via both methods. The rms deviation of the "true" strength function (calculated including the

signs of γ) and the approximate value obtained by ignoring the cross terms were N (% deviation) = 100 (10%), 50 (15%), 30 (21%), 20 (27%), 10 (50%). [In the present data, the $l=1, J=2$ states ($N=24$) are the most suitable for analysis. Unfortunately, the transformation for $l=1, J=2, s=1$ and 2 has an accidental "degeneracy." Both the $p_{1/2}$ and $p_{3/2}$ widths have equally weighted contributions from the $s=1$ and $s=2$ widths and therefore the $p_{1/2}$ and $p_{3/2}$ strength functions are equal.] Without a large number of resonances it is very difficult to accurately determine the splitting of the p -wave strength function via this method.

V. SUMMARY

Differential cross sections for the $^{33}\text{S}(p, p_0), (p, p_1)$, and (p, p_2) reactions were measured in the energy range $E_p=1.20-3.77$ MeV with an overall energy resolution of 350 eV. Resonance parameters were extracted for 144 levels with a multilevel, multichannel R -matrix code. There are now some 230 levels in ^{34}Cl with known parity, including 120 new levels. Although the overall level density increases approximately exponentially, there are significant local deviations which probably reflect nuclear structure effects. The $l=1$ strength is more than an order of magnitude larger than the $l=0$ strength, and both the s - and p -wave strength functions are strongly energy dependent. Most of the $l=1$ strength is below $E_p \approx 2.6$ MeV and almost all of the $l=0$ strength is above $E_p \approx 2.4$ MeV. A number of analog states were identified, but several ambiguities remain. Improved spectroscopy on ^{34}S would facilitate the analog state identification and assist in the long-term goal of establishing a pure and complete level scheme for ^{34}Cl .

ACKNOWLEDGMENTS

The authors would like to thank S. Whetstone and J. R. Erskine for assistance in obtaining the enriched ^{33}S isotope, and P. M. Endt for detailed information on the level assignments in the mass 34 system. The assistance of B. J. Warthen, D. F. Fang, W. K. Brooks, J. S. Bull, and L. James in performing the experiment is appreciated. This work was supported in part by the U.S. Department of Energy, Office of High Energy and Nuclear Physics, Contract Nos. DE-AC05-76ER01067 and DE-FG05-88ER40441.

*Present address: Department of Physics, U.S. Naval Academy, Annapolis, MD 21402.

¹G. Adams, E. G. Bilpuch, G. E. Mitchell, R. O. Nelson, and C. R. Westerfeldt, *J. Phys. G* **10**, 1747 (1984).

²D. F. Fang, E. G. Bilpuch, C. R. Westerfeldt, and G. E. Mitchell, *Phys. Rev. C* **37**, 28 (1988).

³P. M. Endt and C. van der Leun, *Nucl. Phys. A* **310**, 1 (1978).

⁴P. M. Endt (private communication).

⁵J. R. Erskine, D. J. Crozier, J. P. Schiffer, and W. P. Alford,

Phys. Rev. C **3**, 1976 (1971).

⁶H. Brunnader, J. C. Hardy, and J. Cerny, *Nucl. Phys. A* **137**, 487 (1969).

⁷A. K. Hyder, Jr. and G. I. Harris, *Phys. Rev. C* **4**, 2046 (1971).

⁸F. B. Waanders, J. P. L. Reinecke, K. N. Jacobs, J. J. A. Smit, M. A. Meyer, and P. M. Endt, *Nucl. Phys. A* **411**, 81 (1983).

⁹P. W. M. Glaudemans, L. Eriksson, and J. A. R. Werkhoven, *Nucl. Phys.* **55**, 559 (1964).

¹⁰D. Dassié, F. Leccia, and P. Mennrath, *Nucl. Phys. A* **276**,

- 260 (1977).
- ¹¹D. Dassié, F. Leccia, and P. Mennrath, Nucl. Phys. A **276**, 279 (1977).
- ¹²R. U. Haq, A. Pandey, and O. Bohigas, Phys. Rev. Lett. **48**, 1086 (1982).
- ¹³O. Bohigas and M. J. Giannoni, in *Mathematical and Computational Methods in Nuclear Physics*, Vol. 209 of *Lecture Notes in Physics*, edited by J. S. Dehasa, J. M. G. Gomez, and A. Polls (Springer-Verlag, Berlin, 1983), p. 1.
- ¹⁴T. von Egidy, A. N. Behkami, and H. H. Schmidt, Nucl. Phys. **A454**, 109 (1986).
- ¹⁵A. Y. Abul-Magd and H. A. Weidenmüller, Phys. Lett. B **162**, 223 (1985).
- ¹⁶T. von Egidy, H. H. Schmidt, and A. N. Behkami, Nucl. Phys. **A481**, 189 (1988).
- ¹⁷P. M. Endt, P. de Witt, and C. Alderliesten, Nucl. Phys. **A459**, 61 (1986).
- ¹⁸G. E. Mitchell, E. G. Bilpuch, P. M. Endt, and J. F. Shriner, Jr., Phys. Rev. Lett. **61**, 1473 (1988).
- ¹⁹C. R. Westerfeldt, R. O. Nelson, E. G. Bilpuch, and G. E. Mitchell, Nucl. Instrum. Methods A **270**, 467 (1988).
- ²⁰W. A. Sterrenberg, G. van Middelkoop, J. A. G. de Raedt, A. Halthuizen, and A. J. Rutten, Nucl. Phys. **A306**, 157 (1978).
- ²¹G. J. L. Nooren and C. van der Leun, Nucl. Phys. **A423**, 197 (1984).
- ²²A. M. Lane and R. G. Thomas, Rev. Mod. Phys. **30**, 257 (1958).
- ²³R. O. Nelson, E. G. Bilpuch, and G. E. Mitchell, Nucl. Instrum. Methods A **236**, 128 (1985).
- ²⁴J. W. Olness, W. Haeberli, and H. W. Lewis, Phys. Rev. **112**, 1702 (1958).
- ²⁵C. van der Leun and P. M. Endt, Nucl. Phys. **53**, 540 (1964).
- ²⁶J. G. van der Baan and B. R. Sikora, Nucl. Phys. **A173**, 456 (1971).
- ²⁷D. J. Crozier, Nucl. Phys. **A198**, 209 (1972).
- ²⁸E. G. Bilpuch, A. M. Lane, G. E. Mitchell, and J. D. Moses, Phys. Rep. C **28**, 145 (1976).
- ²⁹S. A. A. Zaidi and S. Darmodjo, Phys. Rev. Lett. **19**, 1446 (1967).
- ³⁰H. L. Harney, Nucl. Phys. **A119**, 591 (1968).
- ³¹H. L. Harney and H. A. Weidenmüller, Nucl. Phys. **A139**, 241 (1969).
- ³²J. D. Moses, Ph.D. thesis, Duke University, 1969 (unpublished).
- ³³S. Hinds (private communication quoted in Ref. 3).
- ³⁴P. M. Endt and C. van der Leun, Atomic Data Nuclear Data Tables **13**, 67 (1974).
- ³⁵B. H. Wildenthal, J. B. McGrory, E. C. Halbert, and H. D. Graber, Phys. Rev. C **4**, 1708 (1971).
- ³⁶B. H. Wildenthal, E. C. Halbert, J. B. McGrory, and T. Kuo, Phys. Rev. C **4**, 1266 (1971).
- ³⁷F. C. Erné, Nucl. Phys. **84**, 91 (1966).
- ³⁸J. E. Lynn, *The Theory of Neutron Resonance Reactions* (Clarendon, Oxford, 1968).
- ³⁹Y. Ozawa and E. Arai, Z. Phys. A **323**, 381 (1986).